Article

Transparent and water-resistant composites prepared from acrylic resins ABPE-10 and acetylated NFC as FOLED substrate

Xueping Song[1,2†], Shuang Yang[1,2†], Xiuyu Liu[1,3], Min Wu[1,2], Yao Li[4], Shuangfei Wang[1,2*]

1 College of Light Industry and Food Engineering, Guangxi University, Nanning, 530004, PR China；sx_ping@163.com (X.S.);18242364407@163.com (S.Y.); wumin@gxu.edu.cn (M.W.)

2 Guangxi Key Laboratory of Clean Pulp & Papermaking and Pollution Control, Nanning 530004, PR China

3 Department of Chemical and Paper Engineering, Western Michigan University, Kalamazoo, MI 49008-5200, USA；13878171739@163.com (X.L.)

4 Guangxi Vocation ＆ Technical Institute of Industry, Nanning 530004, PR China; 601504088@qq.com (Y.L.)

* Correspondence: 574517745@qq.com; Tel.:+86-159-9434-1859

† These authors contributed equally to the work.

Abstract: The ANFC/ABPE-10 composite film was prepared by ABPE-10 impregnating into ANFC films under negative pressure. And the composite film had meted high performance FOLED substrate requirement even when ANFC dosage was high for approximately 70%, which was consistent with for low cost efficiency, recyclability, and environmentally friendly. The enhanced properties of ANFC films were mainly because of the nature of ABPE-10 itself and the IPN structure formed between ABPE-10 and ANFC film. The transparency of composite films with different ANFC dosage was significantly increased from 67% to 88% by UV-Vis analysis. The composite film inherited the properties of AFNC, obtaining low CTE characteristics and ductile compact structure. The contact angles of ANFC films increased by 102% from 49.2° to 102.9°after dipping ABPE-10. Additionally, the composite films had outstanding mechanical properties such as tensile strength 173.72 MPa, Young's modulus 4.06 GPa, and elongation at break 5.81%.

Keywords: Acetylated nanofibrillated cellulose; Acrylic resins ABPE-10; Composite films; Flexible organic light-emitting device substrate; Interpenetrating polymer network

1. Introduction

Organic light-emitting diode (OLED) provide unique features such as wide viewing angle, high efficiency, low power consumption, high response speed, and low cost, which make to develop highly portable and flexible OLED possible [1,2]. Flexible OLEDs are typically made of the anode, cathode, and organic material films, including electron injection layer, organic emitting layer, hole injection layer between anode and cathode, as well as at least a transparent electrode in order to get the shiny surface [3,4]. Flexible organic light-emitting diode (FOLED) has broad application prospects in information, energy, healthcare, defense, and other fields because of its flexible, high efficiency, and low fabrication cost [5]. Meanwhile, FOLED display will have a profound impact on the application of wearable and portable devices, and will be widely used with the continuous development of personal intelligent terminals [6]. With the growing sophistication of organic light-emitting materials and device technologies, FOLED is regarded as the most promising technology for future displays [5,7].

FOLED is fabricated based on flexible substrate, and is operated in flexible substrate, so the FOLED substrate is a very important part of flexible display device. It needs to provide mechanical support for the equipment, at the same time to facilitate processing photonic and electronic to achieve the specific performance of FOLED equipment, thus the quality of the substrate will ultimately determine the performance of device, life expectancy and production methods. FOLED substrate should have the advantages of smooth, flat, good dimensional stability, high flexibility, good thermal stability, high transparency, and barrier properties [7]. What's more, substrate materials would have an impact on the following processes: electrode deposition, barrier coating, patterning exposure, and thin-film transistor fabrication. Therefore, how to select the proper substrate materials is very critical. In the current FOLED substrates, some synthetic soft polymer matrix are expected to replace the glass substrate, while the large coefficient of thermal expansion (CTE) limit their use. Cellulose is the most abundant renewable raw materials on earth. The nanofibrillated cellulose (NFC) that is prepared from natural fibers via mechanical grinding is composed of aggregate of linear microfibrils with higher aspect ratio. It has the tendency of self-linking through hydrogen bonding interaction between fibers, and the three-dimensional rigid network can be formed within matrix [8]. At the same time, NFC has the advantages of good flexibility, non-friable, low CTE（8×10^{-6} /K）, light weight（density1.5 g/cm^3）, large surface area （>50 m^2/g）, high mechanical properties，and biodegradable, compared with conventional glass materials. What's more, the thin film prepared from NFC is transparent and has high strength [9], which has great application potential in high technology fields such as conductive NFC film [10] and electronic substrate [11]. When the addition amount of NFC is low (≤5%), NFC composites as FOLED substrates still has superior thermal stability, mechanical property, barrier property, and recyclability [12]. In addition, the sheet-by-sheet processing of FOLED substrate can be replaced by large-scale roll-to-roll processing [13]. Therefore, the cost-efficient and environmentally friendly FOLED substrate produced by NFC is attracting intensive research and commercial interesting.

Our previous studies also found that acetylated nanofibrillated cellulose (ANFC) films as FOLED substrates had many advantages such as smooth surface, high flexibility, good thermal properties, and mechanical properties. However, the light transmittance of NFC films was about 70% and had not reached the requirement of FOLED substrates 80% [7], and its water resistance also needed to be enhanced. Acrylic resins ABPE-10 is a kind of colorless, transparent, light-cure, and water-insoluble resin. Compared with the traditional heat cure, light cure technology has the characteristics of fast curing speed, high production efficiency, good physical mechanical properties, and curing at room temperature [14]. Also, the prices of light cure equipment and energy consumption are low, so acrylic resins ABPE-10 is known as an environmentally friendly green material. Okahisa et al. [11] impregnated NFC film in acrylic resins and tetrahydrocyclopentadiene dimethacrylate，and obtained the composite material with high transparency. Nogi and Yano et al. [15,16] prepared flexible substrate by compositing bacterial-cellulose nanofibers films and acrylic resins，also the nanocomposites had excellent performance in optical properties, dimensional stability, and thermal performance. However, these studies rarely describe the combination relationship between ANFC film and acrylic resins ABPE-10, as well as rarely report how to improve the transparency of NFC films produced by mechanically ground NFC for preparing the highly transparent FOLED substrates. Furthermore, the combination of ANFC film and ABPE-10 to improve the water resistance of ANFC membranes as FOLED substrates has also been rarely studied.

The ABPE-10 contains carboxylic acid ester and phenyl structure (in Fig 1), belonging to the amphiphilic substance. The carboxylic acid ester structure of ABPE-10 can form hydrogen bonding with the hydroxyl groups (-OH) in the NFC, enhancing the binding between NFC film and ABPE-10，and improving the evenness of ABPE-10 on the surface of NFC film. On the one hand, the phenyl structure of ABPE-10 after drying can also improve the oxidation resistance and water resistance of FOLED substrate. Additionally，acrylic resins ABPE-10 contains double functional groups (-CH=CH$_2$) structure, which can accelerate UV-light polymerization speed. In order to further improve the light performance, smoothness, and water resistance of FOLED substrate based on

ANFC, we produced the composites of ANFC/ABPE-10 with high ANFC content by simulating the papermaking process, which would provide a low cost-efficient and environmentally friendly method to prepare FOLED substrate. The ANFC film and ABPE-10 interaction mechanism in composite materials are shown in Fig 1. The acrylic resin ABPE-10 with photoinitiator is dipped and swelled into the ANFC film by negative pressure, and the ABPE-10 polymerized in situ under UV-light crosslinks immediately with ANFC film to form a composite film. The three-dimensional network structure is composed of ANFC network and ABPE network, which are partially interlaced on a molecular scale by hydrogen bonding but not covalently bonded to each other. Thus, the structure of ANFC/ABPE-10 composite film should be interpenetrating polymer network (IPN).

In this study, the ANFC film was impregnated in acrylic resins ABPE-10 under the condition of negative pressure, then was cured by UV-light. Herein, transparent and bendable ANFC/ABPE composite film with high ANFC content (approximately 70%) was prepared as FOLED substrate. The combination relationship between ANFC film and ABPE-10 was illustrated, also the transmittance and water resistance of ANFC film as FOLED substrate were improved.

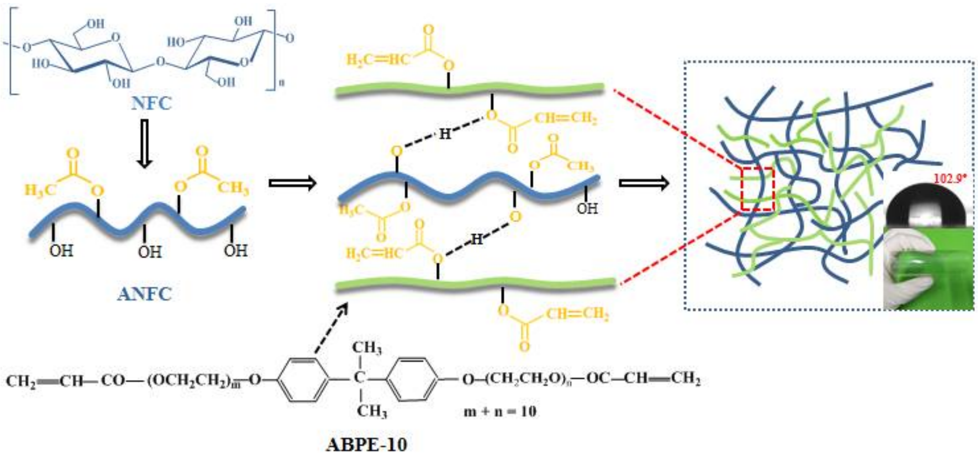

Fig 1. The schematic representation of IPN ANFC/ABPE-10 composite film

2. Materials and Methods

2.1. Materials

Bleached softwood kraft pulp (Pinus khasys), provided by Yun-jiang Forestry & Pulp Mill Co., ltd. (China, Yunnan), contains 96.90% cellulose, 3.50% hemicellulose, and less than 0.1% lignin. It was utilized as the raw material. 1-hydroxycyclohexyl phenyl ketone (analytically pure) as photo initiator, 2-hydroxyethyl acrylate (analytically pure) as reactive diluent, and 2,2-bis[4-(acryloxy polyethoxy) phenyl] propane (acrylic resins ABPE-10) were obtained from the company of Shin Nakamura Chemical Co., Ltd. (Tokyo, Japan).

2.2. Preparation of ANFC

The 3 wt% pulp was ground through a grinder (Super Masscolloider MKZA 10-15JIV; Masuko Sangyo Co., Ltd., Saitama, Japan) at 1,500 rpm for 30 min. Then, the pulp after grinding was diluted to 0.2 wt% pulp suspension and passed through a high-pressure homogenizer (GJJ-0.06/40; Keju fluid equipment manufacturing Co., Ltd., China). The conditions of homogenization were followed: passing 2 times at 0 bars, passing 3 times at 400 bars, and passing 3 times at 600 bars.

The NFC suspension was replaced repeatedly with acetone through vacuum filtration in order to obtain the NFC acetone suspension. Similarly, the NFC toluene suspension was obtained. NFC acetylation was conducted when 25 mL toluene, 20 mL acetic acid, and 0.1 mL perchloric acid were putted into the NFC (83 wt%, 1.0 g bone dry) in sequence. Then, 3 mL acetic anhydride was added to the NFC and was stirred continuously for 1 hour at room temperature. After acetylation, the

 doi:10.20944/preprints201807.0179.v1

ANFC was washed thoroughly with ethanol and distilled water by centrifugal separation, respectively.

2.3. Preparation of ANFC films

The ANFC slurry (0.2, 0.3, 0.4, 0.5, 0.6 g bone dry) was diluted to 0.2 wt%, respectively. And the suspension of diluted ANFC was stirred for 2 hours in order to ensure its dispersion, respectively. Then, the dispersed ANFC was vacuum filtered with G2 sand core funnel (90 mm diameter), which was padded with a layer of hydrophilic polyterafluoroethylene organic filter membrane (0.22 um pore size，90 mm diameter) in advance. The wet ANFC film was taken out together with the organic filter membrane after filtering, covering another organic filter membrane on the other side of ANFC film. Also, the filter papers were covered on the surface of organic filtering films before drying in order to speed up the removal of moisture. The wet ANFC film was pressed from both sides with glass in order to obtain flat film during the drying. Then the film was dried at room temperature for 12 h, and moved to a vacuum drying of 55℃ for 24 h.

2.4. Preparation of IPN ANFC/ABPE composite films

The ANFC films were impregnated in acrylic resins ABPE-10 under a pressure of -0.09 MPa for 12 h. ANFC films were taken out after impregnating, and were used a small coating machine to scrape the extra ABPE-10 on the surface. Then the films were solidified for 3 minutes under the UV light of 1000 W, and the ANFC/ABPE composite films were obtained. At last, the films were balanced more than 24 h under 25℃ and 50% humidity.

2.5. Analysis

2.5.1. Transmission Electron Microscopy (TEM)

The morphology, dimension, and yield of NFC and ANFC were studied by TEM at 100 kV (TECNAI G2 F30, USA). The concentration of NFC and ANFC suspension was diluted to 0.01 wt%, and dispersed for 30 min with ultrasonic, respectively. A small amount of diluted dispersion was carefully dropped on a 200 mesh copper net. After drying at room temperature, sample was dyed with phosphotungstic acid stain for 20 min. The morphology distribution and particle size analysis of samples were carried out using the analyzing software of Nano Measurer 1.2.5.

2.5.2. Determination of acetylation degree

The degree of substitution (DS) of samples were measured by ^{1}H-NMR spectroscopy (Bruker AC III HD600, Germany) [17]. ^{1}H-NMR spectra were measured with an aspectrometer by tetramethylsilane as the internal standard at 256 scanning times and 500 MHz. The sample was dissolved in DMSO-d6, and the DS was calculated according to the formula of Goodlertt [18].

2.5.3. Optical properties

Using the single lens reflex (SLR) camera nikon d7100, the apparent transmittances of films were photographed in a well-lit laboratory. A UV-Vis Spectrometer Lambda 950（PerkinElmer, USA）was used to measure the light transmittance of films in visible wavelength range from 380 nm to 780 nm. The samples were cut into 10 mm×10 mm, and placed at 25 cm from the outlet of the integral sphere.

2.5.4. Apparent morphology

Preprints (www.preprints.org) | NOT PEER-REVIEWED | Posted: 10 July 2018 doi:10.20944/preprints201807.0179.v1

The apparent morphology and tensile fracture-surfaces of the samples were sprayed with gold, then were observed by the field emission scanning electron microscopy (FE-SEM, Hitachi high-technologies corporation SU 8020, Japan).

2.5.5. Contact angle

The contact angles were measured using contact angle meter (DSA100, Germany). The specimen dimensions were 40 mm in length and 10 mm in width. A droplet of distilled water was deposited on the flat film. The contact angle was measured on 3 different points and the average values were calculated.

2.5.6. Thermal performance

The CTE of films was measured by a thermomechanical analyzer (Q400, TA Instruments，U.S.). The measurement conditions were followed: specimens area 25 mm × 3 mm, pull 0.03 N, temperature from 30℃ to 150℃ with the heating rate of 5℃/min. The test was conducted under nitrogen condition, and each sample was circulated three times. The CTE values were determined by the average value of the second run and the third run in order to eliminate the residual stress of the membrane material. CTE values were given as the average of three independent determinations for each sample.

2.5.7. Mechanical properties

The Young's modulus, tensile strength, and elongation at break of the samples were measured using a Shimadzu AG-X testing machine (Kyoto, Japan). The specimen dimensions were 25 mm in length and 3 mm in width. The measurement conditions were followed: load sensor 50 N, gauge length 20 mm, and stretching rate 1 mm/min. Three test samples were measured as well as the data reported were an average of tests.

3. Results and Discussion

3.1. Characteristic analysis of ANFC

TEM micrographs of NFC and ANFC were displayed in Fig 2, and both had a great aspect ratio. The dimensions of NFC and ANFC were obtained by measuring at least 100 individuals from the TEM images. From the Fig 2 (a), there was more than 80% diameter of individual NFC estimated to be within the range of 5-30 nm. Approximately 80% diameter of ANFC had an average between 5-20 nm in Fig 2 (b). The result that acetylation had a little effect on fiber dimension was similar to the finding of Jonoobi et al. [19]. In our earlier study, ANFC film had the best performance when the DS of ANFC was 0.24 shown in Fig 2 (b), and more detailed analysis were described in our previous work [7].

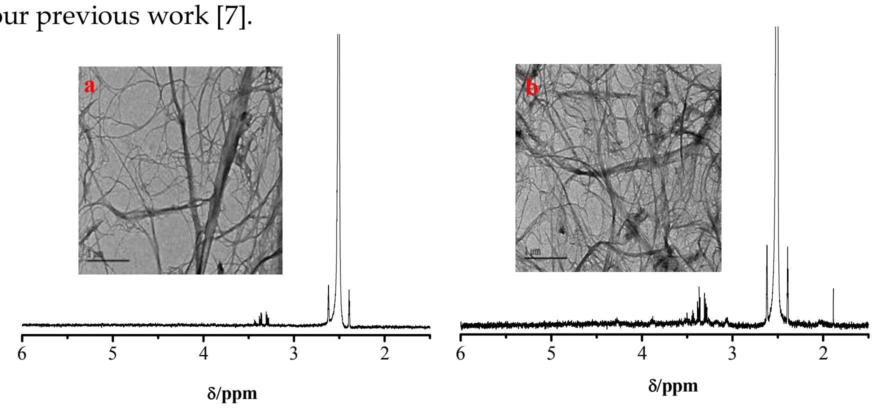

Fig 2. The TEM images and 1H-NMR spectra of (a) NFC and (b) ANFC

3.2. The effects of different ANFC dosages on the optical properties of composite films

Transparency is the most crucial property for bottom emissive displays, and 80% total light transmission of FOLED substrate in the visible light range of 380-780 nm is required [20,21]. The composition and thickness of the composite films are described in the Table 1.

Table 1. The composition and thickness of the films

	NFC (%)	ANFC (%)	ABPE (%)	Thickness (um)
Neat ABPE	—	—	100	42
Neat NFC	100	—	—	42
Neat ANFC	—	100	—	42
ANFC/ABPE	—	53	47	42
ANFC/ABPE	—	59	41	42
ANFC/ABPE	—	68	32	45
ANFC/ABPE	—	74	26	47
ANFC/ABPE	—	77	23	48

The transparency of samples such as neat ANFC film, neat ABPE-10 film, and ANFC/ABPE-10 composite films were illustrated by photographing and UV-Vis Spectrometer analysis (in Fig 3). At the same time, since the ANFC/ABPE-10 composite films with different ANFC dosages had similar apperance images, only the ANFC/ABPE-10 composite film with ANFC dosage 68% was presented as a representative in here. From the Fig 3, although the bee on the red rose of background image could be displayed through these films, the transparency of (a) neat NFC film and (b) neat ANFC film was lower than that of (c) neat ABPE-10 film and (d) ANFC/ABPE-10 composite film, and the transparency of (c) neat ABPE-10 film was slightly higher than that of (d) ANFC/ABPE-10 film.

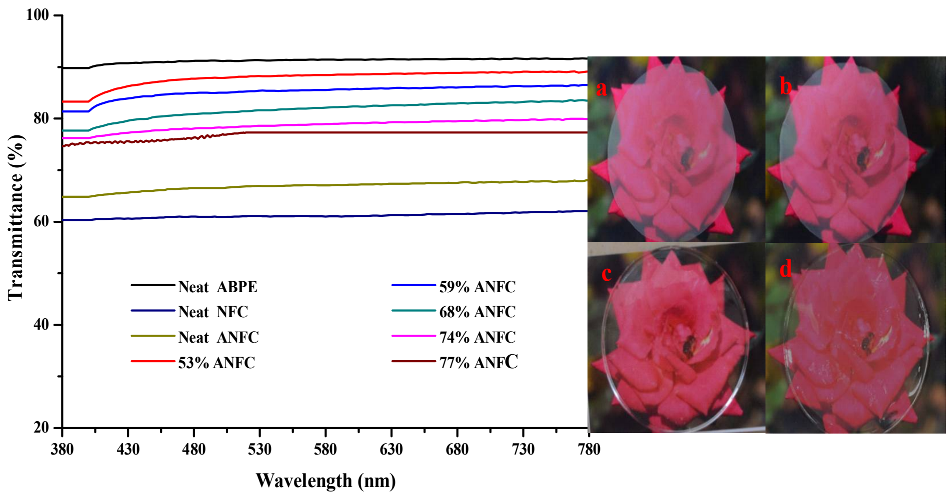

Fig 3. The effects of different ANFC dosages on the transparency of the samples, and the apparent photographs of (a) neat NFC film, (b) neat ANFC film, (c) neat ABPE-10 film, and (d) ANFC/ABPE-10 composite film.

As shown in Fig 3, the transparency of neat NFC film was the lowest compared to others films, followed by the neat ANFC film, indicating that acetylation could slightly improve the transparency of films. The transparency of ANFC/ABPE-10 composite films with different ANFC dosage, compared with that of neat ANFC film, was significantly increased from 67% to 88% at a wavelength of 600 nm at about 45 um thickness, indicating that the combination of ABPE-10 and ANFC was very good for improving the transparency of ANFC film. The main reason was that the ABPE-10 filled the gap of ANFC film and decreased the surface roughness of film, suppressing the

Preprints (www.preprints.org) | NOT PEER-REVIEWED | Posted: 10 July 2018 doi:10.20944/preprints201807.0179.v1

scattering of photons on the surface of film and resulting in the low scattering index [16]. The results were comparable with the findings of Okahisa et al. [11]. Mimicing the light scattering path on different surfaces of films are shown in Fig 4. With the increase of ANFC dosage in the composite film, the transparency of ANFC/ABPE-10 composite films was decreased to varying degrees. It was because that the dense networks structure in films was formed through hydrogen bonding between fibers, which made it difficult to impregnate more acrylic resins ABPE-10 (as shown in Table 1.). The results led ABPE-10 not to well fill the surface porosity of ANFC film and decreased its surface soomthness, and further causing different degrees of light scattering. At the same time, the increase of ANFC dosage led to a slight increase in the thickness of films, eventually also causing a fall in the transparency of composite films. But when the ANFC dosage in composite film was less than 68%, the transparency of ANFC/ABPE-10 composite film was still attained to 80%, meeting the requirement of FOLED substrate. Compared with what Okahisa at al. studied, the ANFC dosage was low around 35%-40% when the transparency of composite films were similar to us [11]. Considering that the cost efficiency, recyclability, and environmentally friendly, the dosage of ANFC should be increased as much as possible without prejudice to transparency requirements.

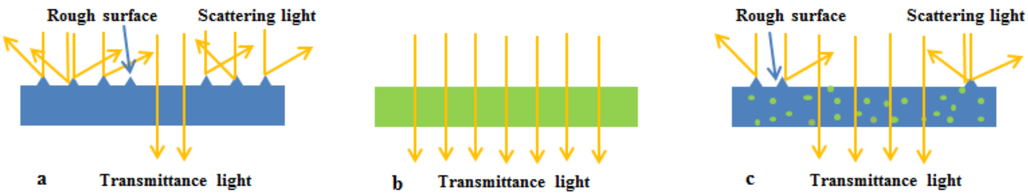

Fig 4. The light scattering path of films: (a) neat ANFC film, (b) neat ABPE-10 film, (c) ANFC/ABPE-10 composite film (68% ANFC)

3.3. The effects of different ANFC dosages on the apparent qualities of composite films

Some surface qualities including roughness, cracks, and cleanliness are important to guarantee the integrity of subsequent barrier and conductive layers. The cracks in substrate may lead to the form of pinholes on the thin films of electrode, creating dark spots in OLEDs. Also, the defects of cracks would be serious when the displays were bent. In order to determine the apparent morphology, stable performance, and the bonding degree of ANFC and ABPE-10，both the apparent morphology and tensile cross-section of films were analyzed by FE-SEM. Since the apparent morphology, tensile cross-section, and contact angle of ANFC/ABPE-10 composite films with different ANFC dosages had similar results, only the ANFC/ABPE-10 composite film with 68% ANFC dosage was present as a representative in here. The results are shown in Fig 5.

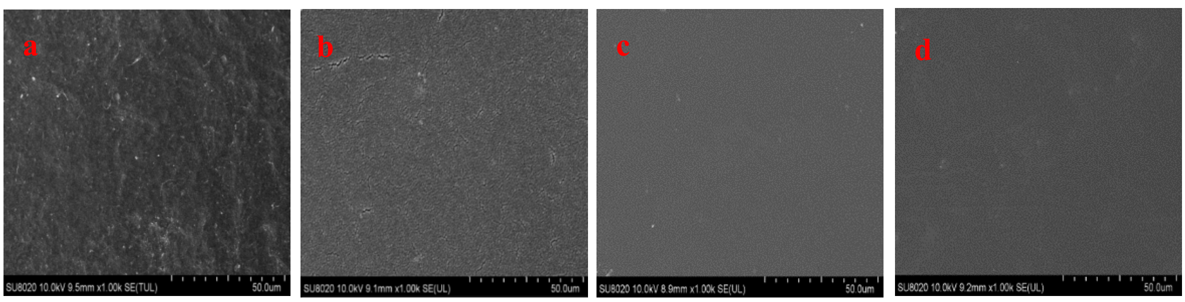

Preprints (www.preprints.org) | NOT PEER-REVIEWED | Posted: 10 July 2018 doi:10.20944/preprints201807.0179.v1

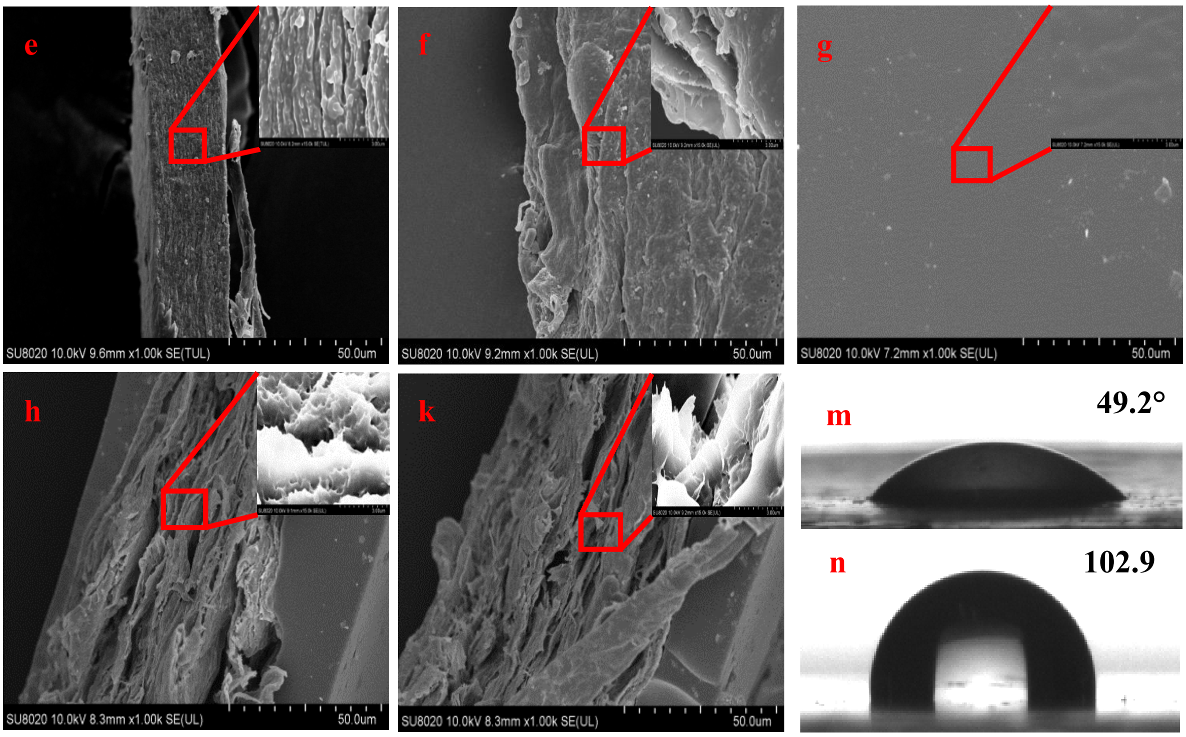

Fig 5. The apparent images of samples: (a) neat NFC film, (b) neat ANFC film, (c) neat ABPE-10 film, (d) ANFC/ABPE-10 composite film (68% ANFC), the tensile cross-section images: (e) neat NFC film, (f) neat ANFC film, (g) neat ABPE-10 film, (h) NFC/ABPE-10 composite film, (k) ANFC/ABPE-10 composite film (68% ANFC),and the contact angle images: (m) neat ANFC film, (n) ANFC/ABPE-10 composite film (68% ANFC).

It could be seen from Fig 5 that the surface of (c) neat ABPE-10 film was most smooth and cleanliness, followed by (d) ANFC/ABPE-10 composite film, under the same magnification of 1.0 K times. Also, some small cracks were observed on the surface of (b) neat ANFC film. Compared with (b) neat ANFC film, the surface smoothness of (d) ANFC/ABPE-10 composite film was greater, and the surface crack had been largely filled, but the surface smoothness was slightly lower than the (c) neat ABPE-10 film. On the basis of these results, we concluded that acrylic resins ABPE-10 could fill the gap of ANFC film well and improved the smoothness of ANFC film. The results further confirmed that acrylic resins ABPE-10 improved the transmittance of the composite film, which was consistent with the observation from Fig 3.

Through the observation for tensile cross-section of (g) neat ABPE-10 film, it could be found that the cross-section was smooth and flat. Also, the fracture direction of the cross-section was consistent and emerged obvious rigidity structure. Under the external load, the ability of such materials to resist being torn and bent was small, leading to rapid expansion of cracks according to the cracks propagation direction. These features of the material presented a typical characteristic of brittle fracture [22]. Thus, neat ABPE-10 film was not suitable for preparing FOLED substrate. Comparing with the image of (e) neat NFC film, the (f) neat ANFC film could be more clearly found that the fracture surface was separated into flakes, scales, and layers, which proved that the fracture was a result of ductile tearing and the ANFC film was tougher material. Fortunately, the composite films prepared by brittle ABPE-10 and ductile NFC/ANFC presented obvious ductile tearing in the Fig 5 (h) and (k), which was due to the fact that the fiber had some outstanding properties including good expansivity, superior flexibility [23], abundance hydrogen bonds, and the three-dimensional network structure of the NFC itself, delaying the breakage. The results would be beneficial to obtain excellent strength performance of FOLED substrate. At the same time, some holes appeared on the cross-section of NFC/ABPE-10 composite film in Fig 5 (h), indicating that the binding of unmodified NFC with ABPE-10 was slightly inferior, compared with the ANFC/ABPE-10 composite film in Fig 5 (k). The compact structure, flakes state, and wiredrawing shape were more obvious and outstanding in ANFC/ABPE-10 composite film than that of Fig 5 (h), which indicated that acetylation improved the compatibility of NFC and ABPE-10. Furthermore, the structure of the composites in Fig 5 (k) showed the IPN structure and presented good interaction and compatibility with the matrix. This structure was often used in the preparation of nanocellulose-based IPN hydrogels with good moisture stability and mechanical performance [24]. Obviously, the ductile compact structure of this substrate would greatly reduce the formation of pinholes on the thin films of electrode, and strengthen the bending performance of displays.

At the same time, acrylic resin ABPE-10 also significantly improved the water resistance of ANFC film. The contact angle of ANFC film increased by 102% from 49.2° to 102.9° after dipping ABPE-10, as shown in Fig 5 (m) and (n). On one hand, the higher water resistance of ANFC/ABPE-10 composite film was due to superior hydrophobic property of acrylic resin ABPE-10. On the other hand, acrylic resin ABPE-10 covered the surface of ANFC film and filled the gaps between nanofibers, which contributed to reduce the hydrophilicity of cellulose by decreasing the exposure of surface hydroxyl. Moreover, the capillary effect of the fiber surface was severely weakened as a result of the decrease of microtube of fiber itself and the interfiber pore. We even ventured to guess that these results should also improve the gas barrier property of ANFC film in a way.

3.4. The effects of different ANFC dosages on the thermal performance of composite films

Thermal stability of substrate is also an important issue that needs to be solved. Improved dimensional stability of composites is desired for FOLED substrate thanks to its varying temperature during application and process. A low CTE is also beneficial to make dimensionally stable designs for devices, and the CTE of FOLED substrate should be less than 20 ppm/K [11,20]. So，the CTE of samples need to be evaluated by thermomechanical analyzer (TMA) and be shown in Table 2.

Table 2. The effects of different ANFC dosages on the CTE of different films

ANFC dosage (g)	CTE (ppm·k-1)
Neat ABPE-10	128.40 ± 2.47
Neat NFC	15.05 ± 0.68
Neat ANFC	5.43 ± 0.35
53% ANFC	15.32 ± 1.10
59% ANFC	15.37 ± 0.75
68% ANFC	13.26 ± 0.58
74% ANFC	11.25 ± 0.48
77% ANFC	10.91 ± 0.50

As shown in Table 2, the CTE of neat ANFC film was about 5.43 ppm/K, and the thermal stability was more excellent compared to that of neat NFC film. The CTE of neat ABPE-10 film was extremely high for 128.40 ppm/K approximately, which would lead to unstable dimensions during application. However, the CTE of the ANFC/ABPE-10 composite films had fallen sharply compared to neat ABPE-10 film, ranging from 128 ppm/K to 11 ppm/K, which could be comparable to glass [25]. Simultaneously, when the dosage of ANFC in ANFC/ABPE-10 composite film was increased from 53% to 77%, the CTE of composite films were slightly decreased. These results indicated that the dosage of ANFC with low CTE characteristics played an important role in the decrease of CTE of composite films. This was because that the thermal stability of composites mainly depended on the thermal properties of material and the enhancer [20]. Additionally, the three-dimensional network structure of composite films was strengthened with the increase of ANFC weight percentage, further causing the variation of composites' density [26], thus limiting the thermal expansion of the composite films.

3.5. The effects of different ANFC dosages on the mechanical properties of composite films

The high mechanical properties of FOLED substrate are of great significance to keeping the robustness and flexibility of FOLED, and meeting the preparation requirement of roll-to-roll [27]. Fig 6 and Fig 7 show the mechanical properties and flexibility of different films，respectively.

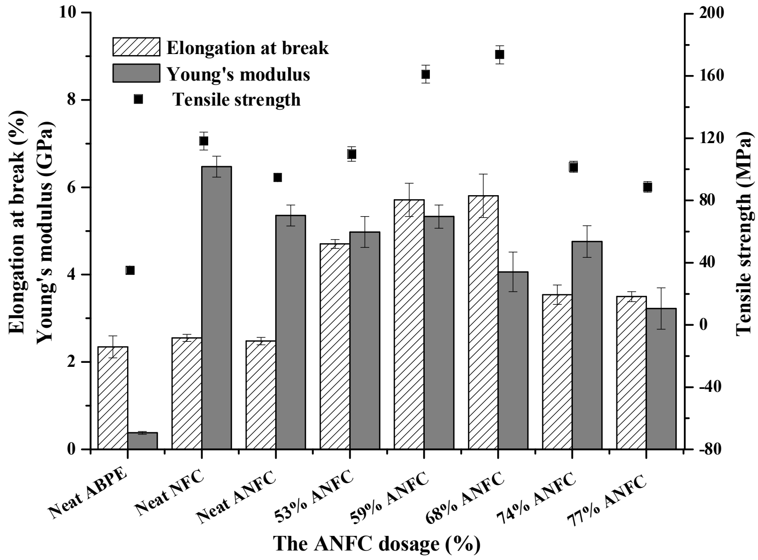

Fig 6. The effects of different ANFC dosages on the mechanical properties of different films

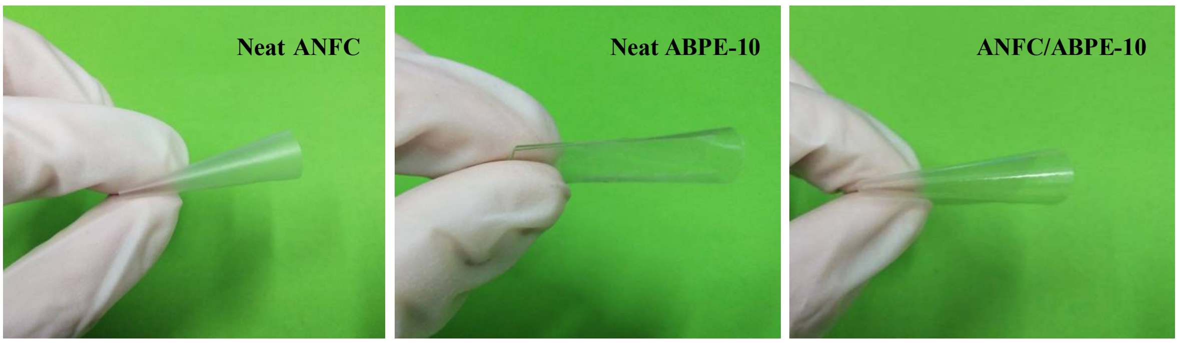

Fig 7. Flexibility of different films

The ultimate strength of composite materials, especially nanocomposites, mainly depends on the nature and volume fraction of the component, and the adhesiveness and compatibility of polymer matrix and additives, known by the study of Dufresne [28]. As shown in Fig 6, compared with the neat ABPE-10 film, the mechanical properties of ANFC/ABPE-10 composite films were improved dramatically. And when ANFC dosage increased to 68%, the tensile strength, Young's modulus, and elongation at break of the composite film increased by 3.94 times, 9.68 times and 1.47 times, respectively. Compared with the neat ANFC film, both tensile strength and elongation at break of ANFC/ABPE-10 composite films were significantly improved. This was mainly due to the fact that the formation of IPN structure between fiber and ABPE-10 strengthened the stability of composite films. Importantly, those tiny pores and cracks on the surface of ANFC film were filled by ABPE-10 when the film was impregnated in ABPE-10 under a certain pressure, enhancing the compactness of film matrix, and thus improving its mechanical properties, which was similar to the findings of Yoko Okahisa [11]. However, when the ANFC dosage was more than 68%, the mechanical properties of composite films had fallen sharply. One of main reasons was that the cracks and holes on the surface of ANFC film could not be well covered with the reduced adhesiveness of ANFC and ABPE-10, with the decreasing of ABPE-10 dosage in the composite film

Preprints (www.preprints.org) | NOT PEER-REVIEWED | Posted: 10 July 2018 doi:10.20944/preprints201807.0179.v1

(shown in table 1), eventually resulting in the non-uniform force and deteriorating the mechanical properties. Additionally, both the neat ANFC film and ANFC/ABPE-10 composite film presented an outstanding flexibility in Fig 7. On the contrary, the flexibility of neat ABPE-10 film was bad, which brought about the breakage of film, which were consistent with the research of Nogi et al. [29]. Notably, this was also supported by the apparent morphology and tensile cross-section of films in Fig 5.

3.6. Performance comparison of different polymer FOLED substrates

Table 3. Performance comparison of different polymers FOLED substrates [16,30,31]

OLED substrates	tensile strength (MPA)	Young's modulus (GPA)	elongation at break (%)	transmittance (%)	CTE (ppm • K-1)
ANFC/ABPE-10 composite film	173.72	4.06	5.81	82.53	13.26
BC/PU composite film	69.50	6.00	1.90	82.00	-
BC/epoxy resin composite film	325.00	20.00	0.02	84.00	6.00
Polyethylene terephthalate	-	2.00-2.70	7.90	83.00	20.00-100.00

Through the experiment results analysis above, we concluded that when ANFC dosage was about 68% in composite film, the performance of FOLED substrate could be maximally improved, the results were: transmittance 82.53 %, contact angle 102.9°, CTE 13.26 ppm/K, tensile strength 173.72 MPa, Young's modulus 4.06 GPa, elongation at break 5.81%, and good flexibility. From Table 3, the CTE of polyethylene terephthalate was very larger than other polymers and was not suitable for substrate requirements. And the transmittance of all polymer FOLED substrates at the wavelength of 600 nm was nearly the same. Meanwhile, the uniform deformation or stable deformation of BC/epoxy resin composite film was poor thanks to its low elongation at break. Thence, the mechanical properties of the ANFC/ABPE-10 composite films were exceedingly excellent, compared to the BC/PU and BC/epoxy resin composite film in Table 3. In spite of the fact that the CTE of ANFC/ABPE-10 composite films was higher than BC/epoxy resin composite film, it was less than 20 ppm • K^{-1} meeting the requirements of the substrate. In summary, considering that the cost efficiency, recyclability, and environmentally friendly, the dosage of ANFC should be increased as much as possible without affecting the properties of FOLED substrate. The ANFC/ABPE-10 composite films prepared in this study combined the following advantages: cheapness, superior thermal stability, great flexibility, good biodegradability, high transparency, good smoothness, as well excellent mechanical performance, and could be used as high performance FOLED substrate.

4. Conclusions

The ANFC/ABPE-10 composite film was prepared by ABPE-10 impregnating into ANFC films under negative pressure. And the performance of the thin composite film (45 um) could maximally be improved and had meted the FOLED substrate requirement when ANFC dosage was high for approximately 70%. The properties of ANFC films were enhanced mainly because of the nature of ABPE-10 itself and the IPN structure formed between ABPE-10 and ANFC film. In fact, the composite films displayed high transparency (up to 80%), low CTE (13.26 ppm/K), and good water resistance. Additionally, the composite films had outstanding mechanical properties such as tensile

 doi:10.20944/preprints201807.0179.v1

strength 173.72 MPa, Young's modulus 4.06 GPa, elongation at break 5.81%. Therefore, we suggest that ANFC/ABPE-10 composite film is potential candidate for FOLED substrate.

Author Contributions: Data Curation and Funding Acquisition, X.S.; Writing-Original Draft Preparation, S.Y.; Writing-Review & Editing, S.Y. and X.S.; Methodology and Resources, X.L.; Software, M.W.; Conceptualization, Y.L.; Supervision and Project Administration, S.W..

Acknowledgments: The project is sponsored by the National Natural Science Foundation of China (21766002), and the Dean project of Guangxi Key Laboratory of Clean Pulp & Papermaking and Pollution Control (KF201603 and ZR201606).

Conflicts of Interest: The authors declare no competing financial interest.

References

1 Salehifar, S.; Shayesteh, M.R.; Hashemian, S. Design and dynamic analysis of a high-speed organic light-emitting diode. *J. Electron. Mater.* **2018**, *47*, 1279-1284. **DOI:** 10.1007/s11664-017-5911-0

2 Saikia, D.; Sarma, R. Organic light-emitting diodes with a perylene interlayer between the electrode-organic interface. *J. Electron. Mater.* **2018**, *47*, 737-743. **DOI:** 10.1007/s11664-017-5806-0

3 Legnani, C.; Vilani, C.; Calil, V.L.; Barud, H.S.; Quirino, W.G.; Achete, C.A.; Ribeiro, S.J.L.; Cremona, M. Bacterial cellulose membrane as flexible substrate for organic light emitting devices. *Thin Solid Films* **2008**, *517*, 1016-1020. **DOI:** 10.1016/j.tsf.2008.06.011

4 Zardetto, V.; Brown, T.M.; Reale, A.; Di Carlo, A. Substrates for flexible electronics: A practical investigation on the electrical, film flexibility, optical, temperature, and solvent resistance properties. *J. Polym. Sci. B: Pol. Phys.* **2011**, *49*, 638-648. **DOI:** 10.1002/polb.22227

5 Geffroy, B.; Le Roy, P.; Prat, C. Organic light-emitting diode (oled) technology: Materials, devices and display technologies. *Polym. Int.* **2006**, *55*, 572-582. **DOI:** 10.1002/pi.1974

6 Luo, Y.; Wang, C.; Wang, L.; Ding, Y.; Li, L.; Wei, B.; Zhang, J. Flexible organic light-emitting diodes with enhanced light out-coupling efficiency fabricated on a double-sided nanotextured substrate. *Acs Appl. Mater. Inter.* **2014**, *6*, 10213-10219. **DOI:** 10.1021/am501521p

7 Yang, S.; Xie, Q.; Liu, X.; Wu, M.; Wang, S.; Song, X. Acetylation improves thermal stability and transmittance in foled substrates based on nanocellulose films. *RSC Adv.* **2018**, *8*, 3619-3625. **DOI:** 10.1039/c7ra11134g

8 Khan, A.; Huq, T.; Khan, R.A.; Riedl, B.; Lacroix, M. Nanocellulose-based composites and bioactive agents for food packaging. *Crit. Rev. Food Sci.* **2014**, *54*, 163-174. **DOI:** 10.1080/10408398.2011.578765

9 Aulin, C.; Salazar-Alvarez, G.; Lindstrom, T. High strength, flexible and transparent nanofibrillated cellulose-nanoclay biohybrid films with tunable oxygen and water vapor permeability. *Nanoscale* **2012**, *4*, 6622-6628. **DOI:** 10.1039/c2nr31726e

10 Nystrom, G.; Mihranyan, A.; Razaq, A.; Lindstrom, T.; Nyholm, L.; Stromme, M. A nanocellulose polypyrrole composite based on microfibrillated cellulose from wood. *J. Phys. Chem. B* **2010**, *114*, 4178-4182. **DOI:** 10.1021/jp911272m

11 Okahisa, Y.; Yoshida, A.; Miyaguchi, S.; Yano, H. Optically transparent wood-cellulose nanocomposite as a base substrate for flexible organic light-emitting diode displays. *Compos. Sci. Technol.* **2009**, *69*, 1958-1961. **DOI:** 10.1016/j.compscitech.2009.04.017

12 Oksman, K.; Mathew, A.P.; Bondeson, D.; Kvien, I. Manufacturing process of cellulose whiskers/polylactic acid nanocomposites. *Compos. Sci. Technol.* **2006**, *66*, 2776-2784. **DOI:** 10.1016/j.compscitech.2006.03.002

13 Nogi, M.; Yano, H. Optically transparent nanofiber sheets by deposition of transparent materials: A concept for a roll-to-roll processing. *Appl. Phys. Lett.* **2009**, *94*. **DOI:** 10.1063/1.3154547

14 Narayanan, V.; Scranton, A.B. Photopolymerization of composites. *Trends Polym. Sci.* **1997**, *5*, 415-419. **DOI:** ir.uiowa.edu/cbe_pubs/61

15 Masaya, N.; Hiroyuki, Y. Transparent nanocomposites based on cellulose produced by bacteria offer potential innovation in the electronics device industry. *Adv. Mater.* **2008**, *20*, 1849-1852. **DOI:** 10.1002/adma.200702559

16 Yano, H.; Sugiyama, J.; Nakagaito, A.N.; Nogi, M.; Matsuura, T.; Hikita, M.; Handa, K. Optically transparent composites reinforced with networks of bacterial nanofibers. *Adv. Mater.* **2005**, *17*, 153-155. **DOI:** 10.1002/adma.200400597

17 Sun, X.; Lu, C.; Zhang, W.; Tian, D.; Zhang, X. Acetone-soluble cellulose acetate extracted from waste blended fabrics via ionic liquid catalyzed acetylation. *Carbohyd. Polym.* **2013**, *98*, 405-411. **DOI:** 10.1016/j.carbpol.2013.05.089

18 Goodlett, V.W.; Dougherty, J.T.; Patton, H.W. Characterization of cellulose acetates by nuclear magnetic resonance. *J. Poly. Sci. A: Polym. Chem.* **1971**, *9*, 155-161. **DOI10**.1002/pol.1971.150090114

19 Jonoobi, M.; Harun, J.; Mathew, A.P.; Hussein, M.Z.B.; Oksman, K. Preparation of cellulose nanofibers with hydrophobic surface characteristics. *Cellulose* **2010**, *17*, 299-307. **DOI:** 10.1007/s10570-009-9387-9

20 Choi, M.-C.; Kim, Y.; Ha, C.-S. Polymers for flexible displays: From material selection to device applications. *Prog. Polym. Sci.* **2008**, *33*, 581-630. **DOI:** 10.1016/j.progpolymsci.2007.11.004

21 Ummartyotin, S.; Juntaro, J.; Sain, M.; Manuspiya, H. Development of transparent bacterial cellulose nanocomposite film as substrate for flexible organic light emitting diode (oled) display. *Ind. Crop. Prod.* **2012**, *35*, 92-97. **DOI:** 10.1016/j.indcrop.2011.06.025

22 Salazar, A.; Prolongo, S.G.; Rodriguez, J. Fracture properties of epoxy/poly(styrene-co-allylalcohol) blends. *J. Appl. Polym. Sci* **2007**, *106*, 3227-3236. **DOI:** 10.1002/app.26811

23 Song, X.; Jiang, Y.; Rong, X.; Wei, W.; Wang, S.; Nie, S. Surface characterization and chemical analysis of bamboo substrates pretreated by alkali hydrogen peroxide. *Bioresource Technol.* **2016**, *216*, 1098-1101. **DOI:** 10.1016/j.biortech.2016.06.026

24 Naseri, N.; Deepa, B.; Mathew, A.P.; Oksman, K.; Girandon, L. Nanocellulose-based interpenetrating polymer network (ipn) hydrogels for cartilage applications. *Biomacromolecules* **2016**, *17*, 3714-3723. **DOI:** 10.1021/acs.biomac.6b01243

25 Sharma, G.; Arya, S.K.; Singh, K. Optical and thermal properties of glasses and glass-ceramics derived from agricultural wastes. *Ceram. Int.* **2018**, *44*, 947-952. **DOI:** 10.1016/j.ceramint.2017.10.027

26 Poveda, R.L.; Achar, S.; Gupta, N. Thermal expansion of carbon nanofiber-reinforced multiscale polymer composites. *Jom* **2012**, *64*, 1148-1157. **DOI:** 10.1007/s11837-012-0402-5

27 Cordero, N.; Yoon, J.; Suo, Z. Channel cracks in a hermetic coating consisting of organic and inorganic layers. *Appl. Phy. Lett.* **2007**, *90*. **DOI:** 10.1063/1.2713134

28 Dufresne, A.; Dupeyre, D.; Paillet, M. Lignocellulosic flour-reinforced poly(hydroxybutyrate-co-valerate) composites. *J. Appl. Polym. Sci.* **2003**, *87*, 1302-1315. **DOI:** 10.1002/app.11546

29 Nogi, M.; Yano, H. Transparent nanocomposites based on cellulose produced by bacteria offer potential innovation in the electronics device industry. *Adv. Mater.***2008**, *20*, 1849-1852. **DOI:** 10.1002/adma.200702559

30 Pinto, E.R.P.; Barud, H.S.; Silva, R.R.; Palmieri, M.; Polito, W.L.; Calil, V.L.; Cremona, M.; Ribeiro, S.J.L.; Messaddeq, Y. Transparent composites prepared from bacterial cellulose and castor oil based polyurethane as substrates for flexible oleds. *J. Mater. Chem. C* **2015**, *3*, 11581-11588. **DOI:** 10.1039/c5tc02359a

31 Zhu, H.L.; Xiao, Z.G.; Liu, D.T.; Li, Y.Y.; Weadock, N.J.; Fang, Z.Q.; Huang, J.S.; Hu, L.B. Biodegradable transparent substrates for flexible organic-light-emitting diodes. *Energy Environ. Sci.* **2013**, *6*, 2105-2111. **DOI:** 10.1039/c3ee40492g